

The process $p\bar{p} \rightarrow \gamma \pi^0$ within the handbag approach

P. Kroll¹ and A. Schäfer^{2,a}

¹ Fachbereich Physik, Universität Wuppertal, D-42097 Wuppertal, Germany

² Institut für Theoretische Physik, Universität Regensburg, D-93040 Regensburg, Germany

Received: 14 June 2005 / Revised version: 6 September 2005 /

Published online: 26 October 2005 – © Società Italiana di Fisica / Springer-Verlag 2005

Communicated by V. Vento

Abstract. We analyse the exclusive channel $p\bar{p} \rightarrow \gamma \pi^0$, assuming handbag dominance. The soft parts are parametrized in terms of CGLN amplitudes for the $q\bar{q} \rightarrow \gamma \pi^0$ transition and form factors for the $p\bar{p} \rightarrow q\bar{q}$ ones; the latter represent moments of Generalized Distribution Amplitudes. We present a combined fit to Fermilab data from E760 taking simultaneously into account information from other exclusive reactions, especially from $p\bar{p} \rightarrow \gamma\gamma$ data. Overall a nicely consistent picture emerges, such that one can hope, that our theoretical analysis will be reliable also for the kinematics of GSI/FAIR, which, hopefully, will provide much more precise and complete data. Consequently, data from this facility should improve our knowledge both on the proton-antiproton distribution amplitudes and the pion production mechanism.

PACS. 12.38.-t Quantum chromodynamics – 12.38.Bx Perturbative calculations

1 Introduction

The reliable theoretical treatment of hard exclusive processes has been a challenge for QCD for many years. With the advent of the generalized parton distribution formalism [1], a large class of such processes, all involving some hard scale Q^2 , can now be treated on a firm, perturbative QCD basis, absorbing all non-perturbative soft physics in suitable generalized parton distributions. This success is made possible by the dominance of the handbag diagrams in leading twist, as demonstrated in the factorization proofs.

There are other hard exclusive processes for which these rigorous proofs do not apply. Still, however, there are good arguments for the dominance of the handbag contribution in certain regions of phase space also for many of these reactions. Examples of such processes are two-photon annihilations into pairs of hadrons for large but not asymptotically large Mandelstam variables, s , $-t$, $-u$, for applications see [2–4].

The FAIR project at GSI with the HESR antiproton program [5] will offer ideal possibilities to study exclusive channels in $p\bar{p}$ annihilation, *e.g.* $p\bar{p} \rightarrow \gamma\gamma$, the time reversed of the widely studied process $\gamma\gamma \rightarrow p\bar{p}$ [6, 7]. Another very interesting channel is $p\bar{p} \rightarrow \pi^0\gamma$ because rates will be much higher and the amplitude is related by crossing to meson photoproduction $p\gamma \rightarrow \pi^0 p$. The latter process has been recently investigated within the handbag ap-

proach in refs. [8, 9]. It turned out that a leading-twist calculation of the partonic subprocess, which is π^0 photoproduction off quarks, is insufficient. In leading-twist accuracy, *i.e.* considering only the one-gluon exchange mechanism for the generation of the meson, the resulting $\gamma p \rightarrow \pi^0 p$ cross-section is far too small. This parallels observations made in leading-twist calculations of the pion form factor [10]. The results are typically a factor 3 to 4 below the admittedly poor data available at present. In fact the lowest-order Feynman graphs contributing to $\gamma p \rightarrow \pi^0 p$ within the handbag approach are the same as those occurring in the calculation of the pion form factor. Therefore, one has to conclude that for the existing data one is still far from the asymptotic region in which one-gluon exchange dominates and it is necessary to use a more general mechanism for the generation of the meson. Many alternatives and/or corrections to the leading-twist meson generation have been discussed in the literature reaching from higher-twist or power corrections to resummation of perturbative corrections. Still the description of meson generation is a matter of controversy. In order to remedy the situation, a treatment of the subprocess is called for that does not postulate the dominance of any specific meson generation mechanism. Huang *et al.* [9] have proposed such a method. They utilized the covariant decomposition of the $\gamma q \rightarrow \pi^0 q$ amplitudes proposed by Chew, Goldberger, Low and Nambu (CGLN) [11]. This decomposition separates the kinematic and helicity dependences of the subprocess from the dynamics of the meson generation which is embodied in the CGLN invariant functions. Exploiting properties

^a e-mail: andreas.schaefer@physik.uni-r.de

of the invariant functions, various dynamical mechanisms can be identified and consequences discussed. Comparison with experimental data on the ratio of π^+ and π^- photoproduction cross-sections [12] provides evidence for the dominance of one invariant function out of the set of four.

In this work we are going to investigate the corresponding time-like process $p\bar{p} \rightarrow \gamma\pi^0$. As for its space-like partner we will again make use of the CGLN decomposition as, at least for the fixed-target option of FAIR ($s < 30 \text{ GeV}^2$) but possibly also for the collider option ($s < 210 \text{ GeV}^2$), the one-gluon exchange mechanism for meson generation will not dominate. Comparison with existing data from Fermilab [13] at $8.5 \text{ GeV}^2 \leq s \leq 13.6 \text{ GeV}^2$ allows for a critical examination of the handbag characteristics. We will show that, in parallel to the space-like region, there are indications for the dominance of one of the invariant functions. In fact, this function is the $s \leftrightarrow t$ crossed one of the seemingly leading one in the space-like region. Moreover, this function is the one that is fed by the leading-twist mechanism although not sufficiently strongly. Exploiting the crossing properties of the CGLN invariant functions, we are in the position to relate the space- and time-like processes quantitatively. Let us note that for the complementary kinematic regime, namely the production of a virtual photon and a pion into the forward direction, a different factorization scheme was proposed by Pire and Szymanowski [14].

2 The handbag amplitude for $p\bar{p} \rightarrow \gamma\pi^0$

The treatment of proton-antiproton annihilation into photon and meson parallels that of annihilation into two photons, respectively its time-reversed process, two-photon annihilation into $p\bar{p}$, investigated in [3]. Therefore, we can take over many of the results derived in that publication and for clarity we will also use a notation as close as possible to that employed in [3].

Obviously our crucial starting point is the assumption of handbag factorization of the amplitude for the kinematical region $s, -t, -u \gg \Lambda^2$, where Λ is a typical hadronic scale of the order of 1 GeV. In this factorization scheme for which validity arguments have been given in ref. [3], the process amplitudes appear as a product of a hard subprocess, $q^a\bar{q}^a \rightarrow \gamma\pi^0$ and a soft $p\bar{p} \rightarrow q\bar{q}$ transition matrix element which is parametrized by $p\bar{p}$ generalized distribution amplitudes Φ_i^a , $i = A, P, V, S$ introduced in [3] and where a is the flavour of the quark-antiquark pair emitted from the $p\bar{p}$ -pair. The distribution amplitudes Φ_i^a are time-like versions of generalized parton distributions for the proton.

We are interested in large-angle scattering processes. For very high energies the handbag diagram will not dominate, but rather processes like that in fig. 1a [15]. However, this is not a consequence of power counting, but rather of Sudakov suppression, which can only be expected to be effective at really large energies. (A nearly real parton entering or leaving a hard scattering process emits gluon bremsstrahlung. Excluding this part of the cross-section by requiring exclusivity, therefore, leads to

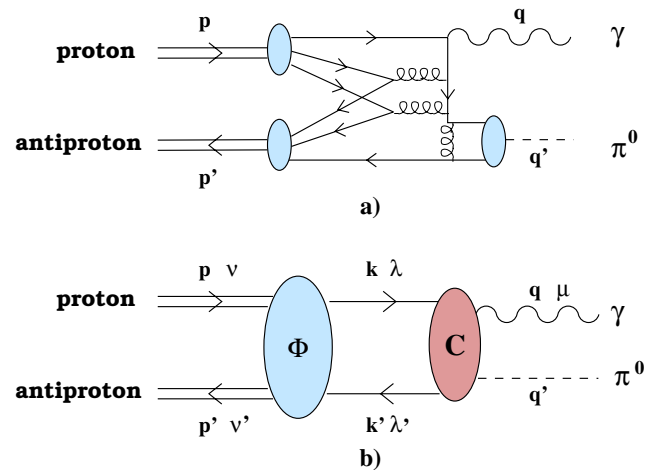


Fig. 1. a) One of the leading-twist contributions at asymptotically large s . The two blobs on the left-hand side represent ordinary proton distribution amplitudes, while the one on the right-hand side is the pion distribution amplitude. b) The handbag contribution at large but non-asymptotic s . The blob on the left-hand side represents the $p\bar{p}$ distribution amplitude, the one on the right-hand side the general dynamics for $q\bar{q} \rightarrow \gamma\pi^0$ parametrized in terms of the CGLN invariant functions. The momenta and helicities of the various particles are indicated.

suppression.) See [16] for details. The asymptotic contribution *à la* Brodsky and Lepage [15] to our process has not yet been worked out. Experience with other processes like $\gamma\gamma \rightarrow p\bar{p}$ [17] or $\gamma p \rightarrow \gamma p$ [18] lets us, however, expect that this contribution to the cross-section is likely to lie way below the experimental points for s of the order of 10 GeV^2 .

As we will follow closely the discussion of two-photon annihilation into $p\bar{p}$, presented in [3], we refrain from presenting all the details of the theoretical analysis, and rather restrict ourselves to a sketch of the main points. We work in a symmetric frame where the momenta of the proton and the antiproton are defined in light-cone coordinates as

$$p = \sqrt{\frac{s}{8}} [1, 1, \sqrt{2}\beta \mathbf{e}_\perp], \quad p' = \sqrt{\frac{s}{8}} [1, 1, -\sqrt{2}\beta \mathbf{e}_\perp], \quad (1)$$

where $\beta = \sqrt{1 - 4m^2/s}$ and m is the mass of the proton. In the following we will work in the massless limit. The transverse direction is characterized by the two-dimensional vector \mathbf{e}_\perp for which we choose $(1, 0)$. The important feature of a symmetric frame in the time-like region is that the skewness is

$$\zeta = p^+/(p^+ + p'^+) = 1/2. \quad (2)$$

The momenta of the photon and the pion read

$$q = \sqrt{\frac{s}{8}} [1 + \sin\theta, 1 - \sin\theta, \sqrt{2}\cos\theta \mathbf{e}_\perp], \\ q' = \sqrt{\frac{s}{8}} [1 - \sin\theta, 1 + \sin\theta, -\sqrt{2}\cos\theta \mathbf{e}_\perp] \quad (3)$$

in our frame of reference which is also a c.m. frame. The scattering angle is denoted by θ and its trigonometric functions are related to the Mandelstam variables by

$$\sin \theta = \frac{2\sqrt{tu}}{s}, \quad \cos \theta = \frac{t-u}{s}. \quad (4)$$

The starting point for the derivation of the handbag amplitude is the expression

$$\begin{aligned} \mathcal{M} = & \sum_a e e_a \int d^4x \int \frac{d^4k}{(2\pi)^4} e^{-ikx} \\ & \times \langle 0 | T \bar{\Psi}_\alpha^a(0) \Psi_\beta^a(x) | p(p) \bar{p}(p') \rangle \mathcal{H}_{\alpha\beta}^a, \end{aligned} \quad (5)$$

where we omitted helicity labels here for convenience. The hard scattering kernel, describing the subprocess $q^a(k) \bar{q}^a(k') \rightarrow \gamma \pi^0$, is denoted by \mathcal{H}^a . The sum runs over the quark flavours $a = u, d, s$; e_a is the corresponding charge in units of the positron charge e . As discussed in detail in [2, 3, 19], the $p\bar{p} \rightarrow q\bar{q}$ transition at large s can only be soft if the outgoing quark and antiquark have small virtualities and each carries approximatively the momentum of the baryon or antibaryon; the deviations of the parton momenta from the hadronic ones in size and direction are of order Λ^2/s . It can be further shown that the dominant Dirac structure of the soft transition matrix element in (5) involves the good components of the quark fields in the parlance of light-cone quantization. The hard scattering amplitudes can be approximatively be calculated with on-shell parton momenta: $H^a = \bar{u}^a \mathcal{H}^a u^a$. This guarantees gauge invariance. Within our calculational scheme we also use the approximation that the proton (antiproton) dominantly emits a valence quark (antiquark). Contributions from the emission of fast sea quarks are expected to be small.

Putting all this together we obtain, in full analogy to the case of $p\bar{p} \rightarrow \gamma\gamma$ [3], the handbag amplitude for the process under consideration (for the sake of legibility explicit helicities are labelled by their signs),

$$\begin{aligned} \mathcal{M}_{\mu 0, \nu \nu'} = & \sum_a \frac{e}{2} e_a \left\{ \left[H_{\mu 0, + -}^a + H_{\mu 0, - +}^a \right] \delta_{\nu - \nu'} F_V^{a*}(s) \right. \\ & + \left[H_{\mu 0, + -}^a - H_{\mu 0, - +}^a \right] \left[2\nu \delta_{\nu - \nu'} (F_A^{a*}(s) + F_P^{a*}(s)) \right. \\ & \left. \left. - \frac{\sqrt{s}}{2m} \delta_{\nu \nu'} F_P^{a*}(s) \right] \right\} + \mathcal{O}\left(\frac{\Lambda^2}{s}\right), \end{aligned} \quad (6)$$

where we make use of the definition of the annihilation form factors in terms of the $p\bar{p}$ distribution amplitudes Φ_i^a as introduced in [3]. Let us note that in [4] such form factors were estimated in a somewhat schematic GPD model. Comparison with experiment shows that this model underestimates, *e.g.*, F_V . Here we fit the form factors directly to experiment:

$$F_i^a(s) = \int_0^1 dz \Phi_i^a\left(z, \zeta = \frac{1}{2}, s, \mu_F^2\right) \quad \text{for } i = V, A, P. \quad (7)$$

In ref. [3] the form factors are defined for the soft transitions $q^a \bar{q}^a \rightarrow p\bar{p}$, while here we consider the time-reversed

transitions. Therefore, the complex conjugated form factors occur here. The fourth form factor or distribution amplitude, the scalar one, decouples in the symmetric frame ($\zeta = \frac{1}{2}$), see [3]. Note that the relations (7) hold for any physical value of the skewness. They also hold for any value of the factorization scale, μ_F^2 , of the distribution amplitudes, since the vector and axial vector currents have zero anomalous dimensions.

Because the incoming proton-antiproton state has no definite C -parity (p and p' are different), one gets a mixture of contributions with form factors of different C -parity, see [3]. F_A^a and F_P^a is related to the C -even part of the $p\bar{p}$ state (coupling to the quark-antiquark pair) and F_V^a to the C -odd part.

To avoid any confusion let us expand a little on this point. The intermediate quark state transforms under C according to

$$C|q(k)\bar{q}(k')\rangle = |\bar{q}(k)q(k')\rangle = -|q(k')\bar{q}(k)\rangle. \quad (8)$$

Consequently, one can construct two states of definite C -parity:

$$\begin{aligned} |C = -\rangle &= 1/\sqrt{2} [|q(k)\bar{q}(k')\rangle + |q(k')\bar{q}(k)\rangle], \\ |C = +\rangle &= 1/\sqrt{2} [|q(k)\bar{q}(k')\rangle - |q(k')\bar{q}(k)\rangle]. \end{aligned} \quad (9)$$

The $\gamma\pi^0$ final state couples to $|C = -\rangle$ only. However, due to kinematics the contribution from $|q(k')\bar{q}(k)\rangle$ is basically zero (there is hardly any quark in the proton with a momentum close to that of the antiproton and vice versa). The remaining state $|q(k)\bar{q}(k')\rangle$ leads then to C -even and C -odd odd contributions on the same footing.

We emphasize that quark-antiquark helicity non-flip does not occur in (6) although there is baryon helicity non-flip. Although we deal with massless quarks, quark helicity non-flip could contribute since we have not specified the mechanism that controls the generation of the meson. While the leading-twist, one-gluon exchange mechanism is pure helicity flip, twist-3 effects, for instance, produce non-flip contributions. Such contributions which are accompanied by helicity non-flip generalized distribution amplitudes and associated form factors [20], have been studied for the corresponding space-like process in [9]. In this respect $p\bar{p}$ annihilation into $\gamma\pi^0$ differs from annihilation into two photons [3]. The subprocess for the latter reaction is pure helicity flip for massless quarks. In parallel to pion photoproduction where quark helicity flip is neglected [9], we assume that quark helicity non-flip contributions are negligible in the time-like region. In principle, this conjecture can be tested by measuring helicity correlations. As we argued above, the dominant contribution to our process comes from the emission of valence (anti)quarks by the (anti)proton. We therefore have to take into account only the two subprocesses $u\bar{u} \rightarrow \gamma\pi^0$ and $d\bar{d} \rightarrow \gamma\pi^0$. By isospin symmetry the weights of these two subprocesses are $C_{\pi^0}^u = 1/\sqrt{2}$ and $C_{\pi^0}^d = -1/\sqrt{2}$, see the discussion in [9]. It is therefore convenient to pull out these weight factors from the subprocess amplitudes, $H^a = C_{\pi^0}^a H$, and absorb them as well as the corresponding fractional charges into the form factors by introducing,

following previous works [3, 8, 9, 19], annihilation form factors specific to $p\bar{p}$ annihilation into a photon and a π^0 ($i = V, A, P$),

$$R_i^{\pi^0} = \frac{1}{\sqrt{2}} \left(e_u F_i^u - e_d F_i^d \right). \quad (10)$$

After this procedure the subprocess amplitudes are flavour independent and we can drop the corresponding superscript.

To proceed we make use of the CGLN covariant decomposition of the subprocess amplitudes [11]:

$$H_{\mu 0, \lambda \lambda'} = \sum_{i=1}^4 \bar{C}_i(s, t) \bar{u}(k, \lambda) \bar{Q}_i v(k', \lambda'), \quad (11)$$

with the manifestly (elm) gauge invariant covariants

$$\begin{aligned} \bar{Q}_1 &= -2\gamma_5 \left[\bar{k} \cdot \epsilon^* q \cdot q' - \bar{k} \cdot q q' \cdot \epsilon^* \right], \\ \bar{Q}_2 &= -2\gamma_5 \left[\bar{k} \cdot q \not{\epsilon}^* - \bar{k} \cdot \epsilon^* \not{q} \right], \\ \bar{Q}_3 &= -\gamma_5 \left[q \cdot q' \not{\epsilon}^* - q' \cdot \epsilon^* \not{q} \right], \\ \bar{Q}_4 &= -\gamma_5 \not{\epsilon}^* \not{q} \end{aligned} \quad (12)$$

encoding the helicity structure of the subprocess. The vector ϵ denotes the polarisation of the photon and

$$\bar{k} = \frac{1}{2} (k - k'). \quad (13)$$

The invariant functions \bar{C}_j depend on the detailed, unknown dynamics. Using the spinor definitions given in ref. [20], eq. (17), one can calculate the helicity amplitudes in terms of these invariant functions. This reveals that \bar{C}_1 and \bar{C}_4 only contribute to the parton non-flip amplitudes in the massless limit which, as just discussed, will be neglected. The other two invariant functions contribute to the helicity flip amplitudes,

$$\begin{aligned} H_{+0, +-}(s, t) &= -\sqrt{\frac{s}{2}} u \left[\bar{C}_2 - \bar{C}_3 \right], \\ H_{+0, -+}(s, t) &= \sqrt{\frac{s}{2}} t \left[\bar{C}_2 + \bar{C}_3 \right]. \end{aligned} \quad (14)$$

The Mandelstam variables in the subprocess may differ from the ones for the full process due to the proton mass, see, for instance, [21]. Here, in this work we will ignore such possible target mass corrections which are of order m^2/s . Inserting (10) and (14) into (6), we obtain the amplitudes

$$\begin{aligned} \mathcal{M}_{+0, \nu \nu'} &= +\frac{e}{2} \sqrt{\frac{s}{2}} \left\{ \left[+ (t - u) \bar{C}_2 - s \bar{C}_3 \right] \delta_{\nu - \nu'} R_V^{\pi^0 *} \right. \\ &\quad + \left[s \bar{C}_2 - (t - u) \bar{C}_3 \right] \left[2\nu \delta_{\nu - \nu'} (R_A^{\pi^0 *} + R_P^{\pi^0 *}) \right. \\ &\quad \left. \left. - \frac{\sqrt{s}}{2m} \delta_{\nu \nu'} R_P^{\pi^0 *} \right] \right\}, \end{aligned} \quad (15)$$

which lead to the $p\bar{p} \rightarrow \gamma \pi^0$ cross-section,

$$\begin{aligned} \frac{d\sigma}{dt} (p\bar{p} \rightarrow \gamma \pi^0) &= \frac{\alpha_{\text{elm}}}{32} s \\ &\times \left\{ |\bar{C}_2(s, t)|^2 \left[\left(\frac{t - u}{s} \right)^2 |R_V^{\pi^0}(s)|^2 + (R_{\text{eff}}^{\pi^0}(s))^2 \right] \right. \\ &\quad + |\bar{C}_3(s, t)|^2 \left[|R_V^{\pi^0}(s)|^2 + \left(\frac{t - u}{s} \right)^2 (R_{\text{eff}}^{\pi^0}(s))^2 \right] \\ &\quad - 2\text{Re} [\bar{C}_2(s, t) \bar{C}_3^*(s, t)] \left(\frac{t - u}{s} \right) \\ &\quad \left. \times \left[|R_V^{\pi^0}(s)|^2 + (R_{\text{eff}}^{\pi^0}(s))^2 \right] \right\}, \end{aligned} \quad (16)$$

neglecting $\mathcal{O}(m^2/s)$ terms. We note that the target mass corrections, being of order Λ^2/s , are not the only power correction to the handbag amplitude (13). There are others, as, for instance, deviations of the parton momenta from the hadronic ones in size and directions which are also of order Λ^2/s (for a more detailed discussion we refer to ref. [3]). At present there is no consistent method of calculating these power corrections in a systematic way, an issue that the handbag approach shares with many other investigations of hard exclusive and inclusive processes. For consistency we therefore neglect target mass corrections throughout this work, which also facilitates the comparison with results from refs. [3, 4, 8, 9] where the same approximation has been made. Judged from Compton scattering [21] the size of the target mass corrections is probably less than 20% for $s \lesssim 10 \text{ GeV}^2$. Since a particular combination of the form factors $R_A^{\pi^0}$ and $R_P^{\pi^0}$ always appears in the cross-section, we introduce an effective form factor,

$$R_{\text{eff}}^{\pi^0} = \left(|R_A^{\pi^0} + R_P^{\pi^0}|^2 + \frac{s}{4m^2} |R_P^{\pi^0}|^2 \right)^{1/2}. \quad (17)$$

These form factors cannot be disentangled anyway, for lack of suitable polarization data. Equations (15), (16) are the $s \leftrightarrow t$ crossed versions of the handbag amplitudes and the cross-section for $\gamma p \rightarrow \pi^0 p$ derived in ref. [9]. There are only some minor modifications for the form factors occurring as a consequence of the specific frame of reference used in the space- and time-like regions. These modifications which have extensively been discussed in ref. [3], are: Instead of vector and tensor generalized distribution amplitudes or form factors it is of advantage to apply the Gordon decomposition to the vector piece in the time-like region and trade the tensor form factor for the scalar one. It then turns out that, in contrast to the space-like region, the scalar form factor decouples in the symmetric frame with $\zeta = 1/2$ while the pseudoscalar one contributes.

As is obvious from eq. (6), the pseudoscalar annihilation form factor $R_P^{\pi^0}$ generates the $p\bar{p} \rightarrow q\bar{q}$ transitions where proton and antiproton have the same helicities while quark and antiquark have opposite ones. This implies parton configurations of the $p\bar{p}$ system with non-zero orbital angular momentum. It is therefore expected that, at large s , the pseudoscalar form factor is suppressed as compared to the other form factors by at least $1/\sqrt{s}$. If so, it will

not dominate over the other terms in eqs. (16), (17) with increasing s .

3 The annihilation form factors

As is obvious from eq. (15), an analysis of the process $p\bar{p} \rightarrow \gamma\pi^0$ at large s , $-t$, $-u$, requires information on the annihilation form factors (10) which encode the physics of the soft $p\bar{p} \rightarrow q\bar{q}$ transition. Presently, the form factors cannot be calculated from first principles in QCD. Also, there is no model calculation available for them currently. Thus, we have to determine the form factors phenomenologically.

Exploiting the universality property of the generalized distribution amplitudes, we can use the form factors that have been determined from an analysis of two-photon annihilations into $p\bar{p}$ pairs within the handbag approach [3]. We however do not use the results of the numerical analysis presented in ref. [3] since we have now at our disposal the very accurate BELLE data on the differential and integrated cross-sections for $\gamma\gamma \rightarrow p\bar{p}$ [7]. These data allow a determination of the vector and effective form factors from a Rosenbluth-type separation. We therefore redo the analysis of the annihilation form factors. In the handbag approach [3] the $\gamma\gamma \rightarrow p\bar{p}$ cross-section is given by an expression which is analogous to the $|\overline{C}_2|$ -term in eq. (16) with form factors defined analogously to eqs. (10) and (17):

$$\frac{d\sigma}{dt}(\gamma\gamma \rightarrow p\bar{p}) = \frac{4\pi\alpha_{\text{elm}}^2}{s^2} \frac{1}{\sin^2\theta} \{ |R_{\text{eff}}^\gamma|^2 + |R_V^\gamma|^2 \cos^2\theta \}. \quad (18)$$

A fit to the BELLE data on the differential cross-section at the highest measured energy ($3 < \sqrt{s} < 4$ GeV, implying an average s of $s_0 = 10.4$ GeV²) and on the integrated cross-sections for $s \geq 8$ GeV² provides¹

$$\begin{aligned} s^2 R_{\text{eff}}^\gamma &= (2.90 \pm 0.31) \text{ GeV}^4 (s/s_0)^{(-1.10 \pm 0.15)}, \\ |s^2 R_V^\gamma| &= (8.20 \pm 0.77) \text{ GeV}^4 (s/s_0)^{(-1.10 \pm 0.15)}, \end{aligned} \quad (19)$$

where the same energy dependence is assumed for both form factors. The fit to the differential cross-section is compared to experiment in fig. 2. The quality of the fit is, with the exception of the data point at $\cos\theta = 0.55$, very good. The failure with this point may be regarded as an indication that the handbag approach is here at its limits. Indeed for $s \simeq 10.4$ GeV² this scattering angle corresponds to $t \simeq -2$ GeV² which is not much larger than Λ^2 . For comparison we also show in fig. 2 the scattering angle dependence of the cross-section in the case that R_{eff}^γ equals R_V^γ (this curve is arbitrarily normalized). Evidently the form factors are different.

¹ The cross-section data in the region of η_c formation is removed from the fit. Possible signals from the P -wave charmonia are not visible in the BELLE data.

In this energy region the BELLE data for the differential cross-section reveal a minimum at a scattering angle of 90°. For lower energies the cross-sections behave differently [7].

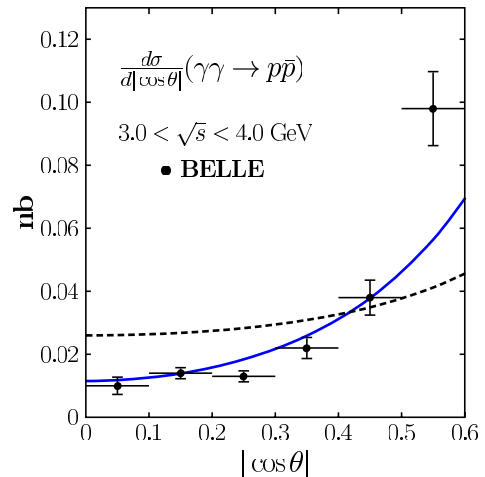


Fig. 2. The differential cross-section for $\gamma\gamma \rightarrow p\bar{p}$ versus $\cos\theta$ at $3.0 < \sqrt{s} < 4.0$ GeV. Data taken from ref. [7]. The solid line represents our fit, while the dashed one shows the angle dependence assuming form factors, $R_{\text{eff}}^\gamma = R_V^\gamma$, for comparison.

The BELLE data exhibit clear evidence for violations of the dimensional counting rules [22], the integrated cross-section falls off faster than s^{-5} resulting in an energy dependence of the annihilation form factors as given in (19) instead of a constant behaviour. As we mentioned above, due to Sudakov suppressions the annihilation form factors are expected to decrease faster than $1/s^2$ for very large s . Recent BELLE measurements [23] on $\gamma\gamma \rightarrow \pi^+\pi^-$ and K^+K^- as well as the JLab measurement [24] of Compton scattering also signal violations of the dimensional counting rules for hard scales of the order of 10 GeV².

We note that the values for the form factors quoted in (19) are somewhat different from the estimate given in ref. [3]. This estimate was based on the the CLEO and VENUS data [6] which are of markedly worse quality than the BELLE data [7] and were only available at the rather low value $s = 7.3$ GeV².

Since we have only protons at our disposal an exact flavour decomposition is not possible. We therefore follow ref. [3] and simplify the expressions by taking a single real constant ρ for the d/u ratio of all proton form factors,

$$F_i^d = \rho F_i^u, \quad i = V, A, P. \quad (20)$$

This ansatz parallels the behaviour of fragmentation functions for $d \rightarrow p$ and $u \rightarrow p$ transitions. In ref. [3] the range of values

$$\rho = 0.25\text{--}0.75 \quad (21)$$

has been considered. We remark that simple quark counting arguments give $\rho = 1/2$ [25]. Combining (20) with the flavour decomposition of the form factors for $\gamma\gamma \rightarrow p\bar{p}$,

$$R_i^\gamma = e_u^2 F_i^u + e_d^2 F_i^d, \quad (22)$$

and neglecting non-valence quark contributions, one finds for the form factors (10) of $\gamma\pi^0$ production

$$R_i^{\pi^0} = \frac{1}{e_u\sqrt{2}} \frac{1 - e_d/e_u\rho}{1 + (e_d/e_u)^2\rho} R_i^\gamma, \quad i = V, A, P. \quad (23)$$

Using the numerical values for the R_i^γ quoted in (19) and adding the errors of the form factors and ρ quadratically, we arrive at the estimate

$$\begin{aligned} |s^2 R_{\text{eff}}^{\pi^0}| &= (3.42 \pm 0.4) \text{ GeV}^4 (s/s_0)^{-1.10 \pm 0.15}, \\ |s^2 R_V^{\pi^0}| &= (9.67 \pm 1.1) \text{ GeV}^4 (s/s_0)^{-1.10 \pm 0.15}. \end{aligned} \quad (24)$$

As we said above, the effective form factor is likely dominated by the axial vector form factor since the pseudoscalar one involves parton orbital angular momentum and is, therefore, expected to be suppressed as compared with the other form factors at large s . An experimental separation of the axial vector and the pseudoscalar from factors requires polarization experiments. The analysis of such observables is beyond the scope of this work. We will only briefly comment on this issue below. For the analysis of cross-sections we only need the effective form factor.

Additional information on the vector form factor is provided by the data on the magnetic proton form factor G_M^p in the time-like region for s up to 14.4 GeV^2 [26]. This form factor is related to the vector form factors (7) by²

$$G_M^p(s) = \sum_{a=u,d} e_a F_V^a(s). \quad (25)$$

The E835 data on the scaled magnetic form factor $s^2 |G_M^p|$ can also be represented by a power law,

$$|s^2 G_M^p| = (2.46 \pm 0.16) \text{ GeV}^4 (s/s_0)^{(-0.75 \pm 0.34)}. \quad (26)$$

An estimate of $R_V^{\pi^0}$ from G_M^p along the same lines as described above, leads to a value smaller than given in (24) [3]. Given the approximations made in the derivation of the handbag contribution [3], there is however no real contradiction.

4 Analysis of the Fermilab (E760) data

Let us turn now to the discussion of the CGLN invariant functions. They have definite behaviour under $t \leftrightarrow u$ crossing [11]:

$$\overline{C}_2(s, t) = \overline{C}_2(s, u), \quad \overline{C}_3(s, t) = -\overline{C}_3(s, u). \quad (27)$$

The invariant functions have dynamical singularities. This can be seen from their leading-twist contributions which are expected to dominate at large s . In this kinematical region the subprocess $q\bar{q} \rightarrow \gamma\pi^0$ is dominated by one-gluon exchange to be calculated in collinear approximation to lowest order of perturbative QCD. One obtains

$$\overline{C}_2^{\text{coll}}(s, t) = \frac{\bar{a}_2^{\text{coll}}}{tu}, \quad \overline{C}_3^{\text{coll}}(s, t) = 0, \quad (28)$$

where

$$\bar{a}_2^{\text{coll}} = 4\pi\alpha_s(\mu_R^2) f_\pi \frac{C_F}{N_c} \langle 1/\tau \rangle_\pi. \quad (29)$$

Here, μ_R^2 is an appropriate renormalization scale, f_π the pion decay constant, $C_F = (N_c^2 - 1)/(2N_c)$ is the usual

² Note that only the form factors (7) are universal in contrast to the flavour combinations occurring in specific processes.

$SU(N_c = 3)$ color factor and the last factor in (29) is the $1/\tau$ moment of the pion distribution amplitude. To leading-twist accuracy also \overline{C}_1 and \overline{C}_4 are zero. These invariant functions control the situation where quark and antiquark have the same helicity. They are only non-zero at twist-3 (or higher) level. As we mentioned in the introduction, the leading-twist, lowest-order pQCD contribution to the subprocess falls short as compared to experiment. It is therefore suggestive to assume that handbag factorization holds and that a more general mechanism than leading-twist, unknown at present, is at work for the generation of the meson and enhances the invariant function \overline{C}_2 sufficiently.

In view of this, let us try now to find a suitable parametrization of the invariant functions. Their singularity structure will not be altered by the inclusion of more complicated dynamical effects such as higher orders of perturbative QCD, transverse degrees of freedom and/or higher twists or power corrections. For instance, by the insertion of an infinite number of fermionic loops in the hard gluon propagator and by interpreting the ambiguities in the resummation of these loop effects—known as infrared renormalons—as a model of higher-twist contributions, an enhancement of the leading twist by a large factor may be obtained [27]. Therefore, a general ansatz for \overline{C}_2 reads

$$\overline{C}_2(s, t) = \frac{\bar{a}_2}{tu} f_2(t, u), \quad (30)$$

where f_2 is a symmetric function of t and u . It may comprise powers of tu/s^2 , *i.e.* powers of $\sin\theta$, or symmetric combinations of $\ln t$ and $\ln u$.

From the leading-twist result (28) one may expect that the invariant function \overline{C}_3 plays only a minor role at s of the order of 10 GeV^2 and may be neglected. This assertion is further supported by an observation made for π^\pm photoproduction [9]: the experimental ratio of these two processes is, within the handbag approach, only understood if $|C_2| \gg |C_3|$ provided quark helicity flip can be neglected. Here, the C_i are the $s \leftrightarrow t$ crossed invariant functions \overline{C}_i . With regard to this observation we will first discuss a scenario with a dominant \overline{C}_2 assuming for it the ansatz (30) with the simplest choice $f_2 \equiv 1$. Taking the estimate (24) for the annihilation form factors we are left with only one free parameter, namely the normalization constant \bar{a}_2 . In general, \bar{a}_2 is a complex number but the cross-section only probes its modulus. The energy and angle dependence of the $p\bar{p} \rightarrow \gamma\pi^0$ cross-section is fixed by the handbag physics.

The differential and integrated cross-section read for this scenario (θ is the angle between incoming proton and the outgoing photon in the center-of-momentum frame.)

$$\begin{aligned} \frac{d\sigma}{d\cos\theta} &= \frac{\alpha_{\text{elm}}}{4s^6} \frac{|\bar{a}_2|^2}{\sin^4\theta} \left[|s^2 R_{\text{eff}}^{\pi^0}|^2 + \cos^2\theta |s^2 R_V^{\pi^0}|^2 \right], \\ \sigma &= \frac{\alpha_{\text{elm}}}{4} \frac{|\bar{a}_2|^2}{s^6} \left[\frac{1}{2} \ln \frac{1+z_0}{1-z_0} \left(|s^2 R_{\text{eff}}^{\pi^0}|^2 - |s^2 R_V^{\pi^0}|^2 \right) \right. \\ &\quad \left. + \frac{z_0}{1-z_0^2} \left(|s^2 R_{\text{eff}}^{\pi^0}|^2 + |s^2 R_V^{\pi^0}|^2 \right) \right], \end{aligned} \quad (31)$$

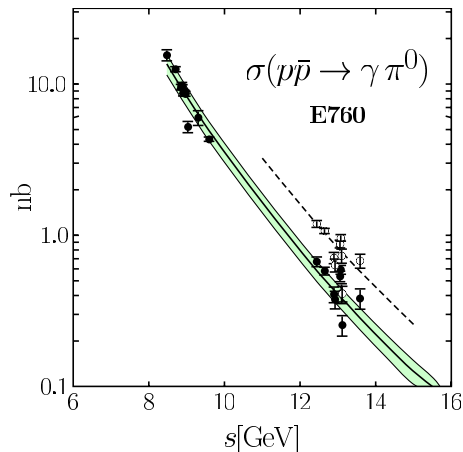


Fig. 3. The integrated cross-section for $p\bar{p} \rightarrow \gamma\pi^0$ versus s . Filled (open) circles: cross-sections integrated over the range $|\cos\theta| = 0$ to z_0 , $z_0 = 0.5$ (0.6). Data taken from [13]. The black lines represent the prediction from the handbag approach with the error bands evaluated from the uncertainties of the annihilation from factors. The dashed line represents a power law fit for $z_0 = 0.6$ with $\sigma \sim (s/s_0)^{8.16 \pm 0.12}$.

where $z_0 = |\cos\theta_0|$ is the limit of integration. With $z_0 = 0.5$ the integrated cross-section is

$$\sigma = 864 \text{ nb GeV}^2 \frac{|\bar{a}_2|^2}{s^6} \left[|s^2 R_{\text{eff}}^{\pi^0}|^2 + 0.096 |s^2 R_V^{\pi^0}|^2 \right]. \quad (32)$$

A fit to the E760 cross-section data provides the value (13.39 ± 0.10) GeV for the parameter $|\bar{a}_2|$. The fit is compared to the data [13] in fig. 3. With regard to the errors of the annihilation from factors quoted in (24), very good agreement of theory and experiment can be claimed. The contribution from J/Ψ formation is very small and can be ignored. We also neglect a possible contribution from the Ψ' . Its decay into $\gamma\pi^0$ has not yet been observed.

For a few energies one may also integrate the E760 data up to $z_0 = 0.6$. For comparison and in order to demonstrate the internal consistency of our numerical analysis, we fit a power law to these data. As can be seen from fig. 3, the fit is in good agreement with the data and yields the value of 8.16 ± 0.12 for the power in perfect agreement with the handbag approach and the form factors (24) estimated from $\gamma\gamma \rightarrow p\bar{p}$. We note in passing that a power of 6 is expected from the dimensional counting rules for our process.

The results from the handbag approach for the differential cross-sections are shown for two energies and for $|\cos\theta| \leq 0.6$ in fig. 4. The excellent agreement between the theoretical results and the E760 data is obvious. Similarly good results are obtained for all energies above 10 GeV^2 , while for lower energies the cross-section data exhibit marked fluctuations which might be indicative of prominent low orbital angular-momentum partial waves. This behaviour of the $p\bar{p} \rightarrow \gamma\pi^0$ cross-section parallels that observed in $p\bar{p} \rightarrow \gamma\gamma$ [6,7] and is the reason why we determined the vector form factor only from BELLE data [7] for the cross-section at $s = 10.4 \text{ GeV}^2$. In order

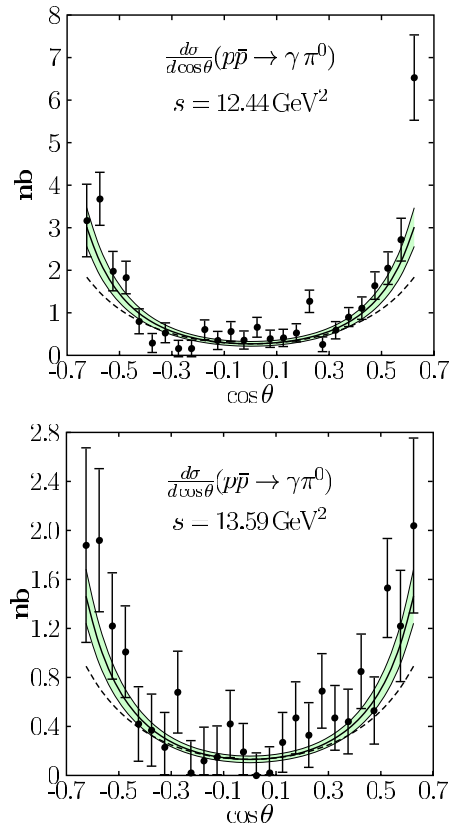


Fig. 4. The differential cross-section for $p\bar{p} \rightarrow \gamma\pi^0$ versus $\cos\theta$ at $s = 12.44 \text{ GeV}^2$ (top) and 13.59 GeV^2 (bottom). Data taken from [13]. The solid lines with the error bands represent the prediction from the handbag approach. For comparison results are also shown where the cross-section behaves $\propto 1/\sin^2\theta$ instead of $\propto 1/\sin^4\theta$ (dashed line).

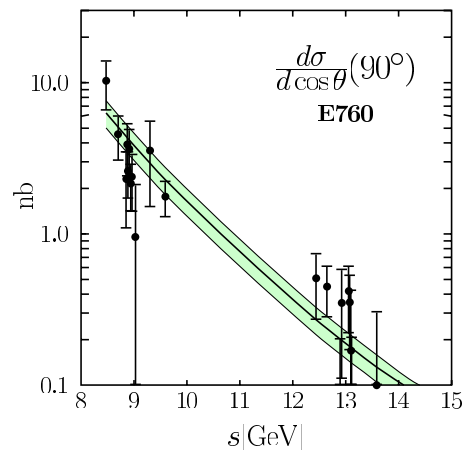


Fig. 5. The differential cross-section for $p\bar{p} \rightarrow \gamma\pi^0$ at 90° versus s . Data, representing the average of the cross-sections in the two bins adjacent to 90° , are taken from [13]. The solid lines with the error bands represent the prediction from the handbag approach.

to further elucidate the structure of the handbag contribution we display the $p\bar{p} \rightarrow \gamma\pi^0$ cross-section at a scattering angle of 90° in fig. 5. Also here we observe fair

agreement between the handbag approach and the data although the errors are substantial.

In fig. 4 we display for comparison also the results of a calculation assuming $f_2 = \sin \theta$ (for simplicity we retain the value of the parameter \bar{a}_2). In this case the angle dependence of the cross-section coincides with that for $p\bar{p} \rightarrow \gamma\gamma$ but it seems to be too weak for the $\gamma\pi^0$ channel, in contrast to the two-photon channel where it is in very good agreement with the BELLE data for $|\cos \theta| \leq 0.5$. Thus, one may conclude that, within errors, there is no need for $f_2 \neq 1$. In other words, an ansatz for the invariant function \bar{C}_2 that resembles the singularity structure of the leading-twist result but with a strength adjusted to experiment, describes the data very well.

From fig. 5 it is also obvious that a scenario $|\bar{C}_3| \gg |\bar{C}_2|$ is in conflict with experiment. The zero of the $t \leftrightarrow u$ antisymmetric invariant function \bar{C}_3 at 90° would lead to a corresponding zero in the differential cross-section which is not seen with the exception of a few energies where a zero is possible within errors³. It goes without saying that a small admixture of \bar{C}_3 to a dominant \bar{C}_2 cannot be ruled out. There is yet another test of the internal consistency of the handbag approach. Our process is related to photoproduction of pions by $s \leftrightarrow t$ crossing as we mentioned occasionally. The form factors are functions of t in the latter case and are known from a recent analysis of nucleon form factors exploiting the sum rules satisfied by generalized parton distributions [16]. Using the invariant function related by $s \leftrightarrow t$ crossing to \bar{C}_2 ,

$$C_2(s, t) = \frac{a_2}{su}, \quad (33)$$

where the Mandelstam variables are now those for photoproduction, one finds fair agreement with the high-energy wide-angle SLAC data [28] if the parameter a_2 is adjusted to these data ($a_2 = 20.3$ GeV). For very large s the parameter a_2 should coincide with $|\bar{a}_2| = 13.39 \pm 0.10$ GeV but at the actual s values of order 10 GeV² this discrepancy is not implausible. Typical differences between time- and space-like values of many quantities are of this size [29]. It is, however, important to realize that the photoproduction data [28] need confirmation.

5 Predictions for FAIR/GSI

Obviously figs. 3 and 5 provide already predictions for the cross-sections to be expected at FAIR. In fig. 6 our prediction for the differential cross-section at $s = 20$ GeV² is shown (the fixed-angle cross-section scales as $s^{8.2 \pm 0.3}$ in our approach). As the discussed luminosities reach up to $2 \cdot 10^4$ nb⁻¹/d for unpolarized reactions and 10^3 nb⁻¹/d for

³ Explicit fits of the \bar{C}_3 scenario to the differential cross-section data, using for instance the ansatz $\bar{C}_3 = \bar{a}_3 \cos \theta/(tu)$, provide results which are too small in the vicinity of 90° as a consequence of this zero. On the other hand, the fit to the integrated cross-section is of the same quality as in the \bar{C}_2 scenario (with $|\bar{a}_3| = 20.05 \pm 0.15$ GeV).

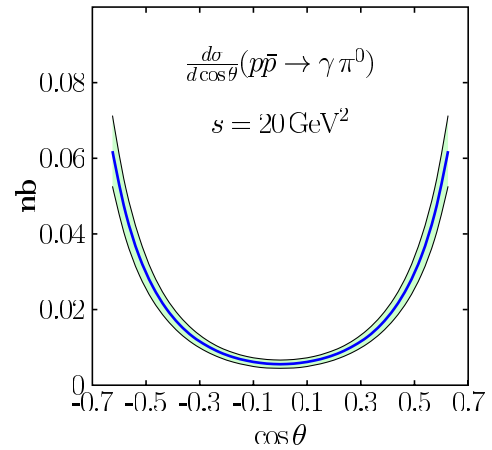


Fig. 6. Cross-section prediction for the FAIR fixed-target energy $s = 20$ GeV².

polarized ones, the data situation will improve drastically, once FAIR is operational [5].

The fact that the protons and antiprotons will be polarized adds very attractive additional possibilities. It allows, *e.g.* to separate $R_A^{\pi^0}$ and $R_P^{\pi^0}$. In analogy to the two-photon channel [3], the helicity correlation A_{LL} between proton and antiproton is given by

$$A_{LL} = \frac{d\sigma(++) - d\sigma(+-)}{d\sigma(++) + d\sigma(+-)} = -\frac{|R_A^{\pi^0} + R_P^{\pi^0}|^2 + \cos^2 \theta |R_V^{\pi^0}|^2 - \frac{s}{4m^2} |R_P^{\pi^0}|^2}{|R_A^{\pi^0} + R_P^{\pi^0}|^2 + \cos^2 \theta |R_V^{\pi^0}|^2 + \frac{s}{4m^2} |R_P^{\pi^0}|^2}, \quad (34)$$

where $d\sigma(\nu\nu')$ is the cross-section for polarized proton-antiproton annihilation.

Our analysis can be easily generalized to other pseudoscalar mesons, *e.g.* to the $\gamma\eta(\eta')$ channel. The only complication arises from the additional $s\bar{s}$ and two-gluon Fock component the η and η' mesons possess. For partons which are emitted nearly collinearly by the proton and antiproton, each carrying a large fraction of its parent's momentum, the strange quarks are likely strongly suppressed. Not much is known about the two-gluon component. There is only some, not very precise information on its leading-twist distribution amplitude from a next-to-leading-order analysis of the $\gamma \rightarrow \eta, \eta'$ transition form factors and the inclusive $\Upsilon \rightarrow \eta' X$ decay [30]. These analyses tell us that to leading-twist accuracy the contribution from the two-gluon Fock component to η' production may be sizeable while it is strongly suppressed in the case of the η . Beyond the leading-twist level the role of the two-gluon contribution is unknown in the case of the η' . Since the η -meson is dominantly a flavour octet state, however, its two-gluon component should be suppressed in any case. In view of this, one can treat the η -meson in the quark-flavour basis and, neglecting the strange component, regard it as $\cos \phi \eta_q$, where ϕ is the usual mixing angle in the quark-flavour basis and η_q is the quark part of the η wave function. The annihilation form factors for

the production of the isoscalar η_q read

$$R_i^{\eta_q} = \frac{1}{\sqrt{2}} \left(e_u F_i^u + e_d F_i^d \right). \quad (35)$$

Their numerical values are somewhat smaller than those for the π^0 given in (24). Up to this difference and a new value of the parameter \bar{a}_2 , the handbag approach then predicts the same energy and angle dependence of the cross-sections for the $\gamma\eta$ channel as for the $\gamma\pi^0$ one. Provided the two-gluon component also plays only a minor role in the case of the η' , the ratio of the $\gamma\eta$ and $\gamma\eta'$ cross-sections is given by

$$\frac{d\sigma(p\bar{p} \rightarrow \gamma\eta)}{d\sigma(p\bar{p} \rightarrow \gamma\eta')} = \cot\phi. \quad (36)$$

In [31] the η - η' mixing angle has been determined to be 39.3° .

Our results for the $\gamma\pi^0$ channel can also be straightforwardly generalized to the γV_L channel, where V_L is a longitudinally polarized vector meson, if we rely again on valence quark dominance. The annihilation form factors for ρ^0 and ω production are the same as given in (24) and (35), respectively. In contrast, ϕ -meson production is expected to be strongly suppressed because of the mismatch of the proton and ϕ -meson valence quarks. The cross-section for the γV_L channel reads

$$\frac{d\sigma^{V_L}}{d\cos\theta} = \frac{\alpha_{\text{elm}}}{4s^6} \frac{|\bar{a}_2^{V_L}|^2}{\sin^4\theta} \left[|s^2 R_V^{V_L}|^2 + \cos^2\theta |s^2 R_{\text{eff}}^{V_L}|^2 \right]. \quad (37)$$

The dependences on the vector and the effective form factors are reversed in this case as a consequence of parity invariance (see, for instance, ref. [8]). We therefore expect a somewhat flatter angular dependence, close to $1/\sin^4\theta$, for the vector meson channels than for $\gamma\pi^0$. The isolation of longitudinally polarized ρ^0 -mesons might be possible with the planned PANDA detector [5].

The generalization to transversally polarized vector mesons, V_T , is more intricate. One has to consider the subprocesses $q\bar{q} \rightarrow \gamma V_T$ with equal and opposite quark and antiquark helicities. In the first case one has to introduce new $p\bar{p}$ distribution amplitudes and, hence, a new set of associated annihilation form factors. These new distribution amplitudes are time-like versions of the helicity flip GPDs introduced in ref. [32]. For opposite quark and antiquark helicities, on the other hand, the formation of the transversally polarized vector meson requires a different mechanism than for longitudinally ones. It is beyond the scope of this work to analyse the processes $p\bar{p} \rightarrow \gamma V_T$.

6 Summary

We have analysed the reaction $p\bar{p} \rightarrow \gamma\pi^0$ for large scattering angles assuming handbag dominance. We obtained a rather satisfying description of the existing Fermilab data from E760. Far more precise data can be expected from FAIR/GSI which also provides the possibility to use polarization variables to separate the different contributions.

Such experiments would contribute to the determination of the generalized distribution amplitudes of the nucleon. It would also allow to clarify the nature of the dominant reaction mechanisms as a function of c.m. energy s . We argue that a similar analysis can be performed without major problems for annihilation in a photon plus either another pseudoscalar meson or a longitudinal vector meson.

We acknowledge helpful discussions with M. Diehl, M. Düren and C. Patrignani and thank the Institute for Nuclear Theory for hospitality, where this project was started during the programme ‘‘GPDs and Exclusive Processes’’. This work was supported by BMBF and, in part, by the Integrated Infrastructure Initiative ‘‘Hadron Physics’’ of the European Union, contract No. 506078.

References

1. For recent reviews see K. Goeke, M.V. Polyakov, M. Vanderhaeghen, Prog. Part. Nucl. Phys. **47**, 401 (2001), hep-ph/0106012; M. Diehl, Phys. Rep. **388**, 41 (2003), hep-ph/0307382. The pioneering papers are: D. Müller, D. Robaschik, B. Geyer, F.M. Dittes, J. Horejsi, Fortschr. Phys. **42**, 101 (1994), hep-ph/9812448; X.D. Ji, Phys. Rev. Lett. **78**, 610 (1997), hep-ph/9603249; A.V. Radyushkin, Phys. Lett. B **380**, 417 (1996), hep-ph/9604317.
2. M. Diehl, P. Kroll, C. Vogt, Phys. Lett. B **532**, 99 (2002), hep-ph/0112274.
3. M. Diehl, P. Kroll, C. Vogt, Eur. Phys. J. C **26**, 567 (2003), hep-ph/0206288.
4. A. Freund, A.V. Radyushkin, A. Schäfer, C. Weiss, Phys. Rev. Lett. **90**, 092001 (2003), hep-ph/0208061.
5. The most up-to-date information can be found on the GSI web-page: <http://www.gsi.de/zukunftprojekt/experimente/index.html>. Of special interest for the actual context are the PAX and PANDA web-pages: http://www.fz-juelich.de/ikp/pax/public_files/tp_PAX.pdf, <http://www.gsi.de/zukunftprojekt/experimente/hesr-panda/index.html>.
6. CLEO Collaboration (M. Artuso *et al.*), Phys. Rev. D **50**, 5484 (1994); VENUS Collaboration (H. Hamasaki *et al.*), Phys. Lett. B **407**, 185 (1997); OPAL Collaboration (G. Abbiendi *et al.*), Eur. Phys. J. C **28**, 45 (2003), hep-ex/0209052.
7. BELLE Collaboration (C.C. Kuo), hep-ex/0503006.
8. H.W. Huang, P. Kroll, Eur. Phys. J. C **17**, 423 (2000), hep-ph/0005318.
9. H.W. Huang, R. Jakob, P. Kroll, K. Passek-Kumericki, Eur. Phys. J. C **33**, 91 (2004), hep-ph/0309071.
10. R. Jakob, P. Kroll, Phys. Lett. B **315**, 463 (1993); **319**, 545 (1993)(E), hep-ph/9306259; S.J. Brodsky, C.R. Ji, A. Pang, D.G. Robertson, Phys. Rev. D **57**, 245 (1998), hep-ph/9705221; B. Melic, B. Nizic, K. Passek, Phys. Rev. D **60**, 074004 (1999), hep-ph/9802204; P. Eden, P. Hoyer, A. Khodjamirian, JHEP **0110**, 040 (2001), hep-ph/0110297.
11. G. Chew, M. Goldberger, F. Low, Y. Nambu, Phys. Rev. **106**, 1345 (1957).
12. JLab Hall A Collaboration (L.Y. Zhu *et al.*), Phys. Rev. Lett. **91**, 022003 (2003), nucl-ex/0211009.

13. Fermilab E760 Collaboration (T.A. Armstrong *et al.*), Phys. Rev. D **56**, 2509 (1997).
14. B. Pire, L. Szymanowski, hep-ph/0504255.
15. G.P. Lepage, S.J. Brodsky, Phys. Rev. D **22**, 2157 (1980).
16. M. Diehl, T. Feldmann, R. Jakob, P. Kroll, Eur. Phys. J. C **39**, 1 (2005), hep-ph/0408173.
17. G.R. Farrar, E. Maina, F. Neri, Nucl. Phys. B **259**, 702 (1985); **263**, 746 (1986)(E).
18. T.C. Brooks, L.J. Dixon, Phys. Rev. D **62**, 114021 (2000), hep-ph/0004143.
19. M. Diehl, T. Feldmann, R. Jakob, P. Kroll, Eur. Phys. J. C **8**, 409 (1999), hep-ph/9811253.
20. M. Diehl, Eur. Phys. J. C **19**, 485 (2001), hep-ph/0101335.
21. M. Diehl, T. Feldmann, H.W. Huang, P. Kroll, Phys. Rev. D **67**, 037502 (2003), hep-ph/0212138.
22. S.J. Brodsky, G.R. Farrar, Phys. Rev. Lett. **31**, 1153 (1973); V.A. Matveev, R.M. Muradian, A.N. Tavkhelidze, Lett. Nuovo Cimento **7**, 719 (1973).
23. BELLE Collaboration (H. Nakazawa *et al.*), Phys. Lett. B **615**, 39 (2005), hep-ex/0412058.
24. E99-114 JLab Collaboration, spokespersons C. Hyde-Wright, A. Nathan, B. Wojtsekhowski, private communications.
25. B.A. Kniehl, G. Kramer, B. Pötter, Nucl. Phys. B **582**, 514 (2000), hep-ph/0010289; F.E. Close, Q. Zhao, Phys. Lett. B **553**, 211 (2003), hep-ph/0210277.
26. E835 Collaboration (M. Ambrogiani *et al.*), Phys. Rev. D **60**, 032002 (1999).
27. A.V. Belitsky, AIP Conf. Proc. **698**, 607 (2004), hep-ph/0307256.
28. R.L. Anderson *et al.*, Phys. Rev. D **14**, 679 (1976).
29. L. Magnea, G. Sterman, Phys. Rev. D **42**, 4222 (1990); A.P. Bakulev, A.V. Radyushkin, N.G. Stefanis, Phys. Rev. D **62**, 113001 (2000), hep-ph/0005085.
30. P. Kroll, K. Passek-Kumericki, Phys. Rev. D **67**, 054017 (2003), hep-ph/0210045; A. Ali, A.Y. Parkhomenko, Eur. Phys. J. C **30**, 183 (2003), hep-ph/0304278.
31. T. Feldmann, P. Kroll, B. Stech, Phys. Rev. D **58**, 114006 (1998), hep-ph/9802409.
32. P. Hoodbhoy, X.D. Ji, Phys. Rev. D **58**, 054006 (1998), hep-ph/9801369; see also [20] above.